

Collocation methods for the
computation of periodic solutions of
delay differential equations

*K. Engelborghs, T. Luzyanina,
K.J. in 't Hout, D. Roose*

Report TW 295, November 1999



Katholieke Universiteit Leuven
Department of Computer Science
Celestijnenlaan 200A – B-3001 Heverlee (Belgium)

Collocation methods for the computation of periodic solutions of delay differential equations

K. Engelborghs, T. Luzyanina,
K.J. in 't Hout†, D. Roose*

Report TW 295, November 1999

Department of Computer Science, K.U.Leuven

Abstract

In this paper we investigate collocation methods for the computation of periodic solutions of autonomous delay differential equations (DDEs). Periodic solutions are found by solving a periodic two-point boundary value problem, which is an infinite-dimensional problem for DDEs, in contrast to the case of ordinary differential equations. We investigate three collocation methods based on piecewise polynomials. We discuss computational issues and show numerical orders of convergence using an extensive number of tests. We compare our numerical results with known theoretical convergence results for initial value problems for DDEs. In particular, we show how super-convergence at the mesh points can be lost or recovered depending on the DDE model under consideration and on the choice of collocation discretisation. We end with a brief discussion of adaptive mesh selection.

Keywords : delay equations, periodic solutions, collocation methods.

AMS(MOS) Classification : Primary : 65J15, Secondary : 65P05.

*On leave from Institute of Mathematical Problems in Biology, RAS, Pushchino, Moscow region, 142292, Russia

†Mathematical Institute, Leiden University, P.O.Box 9512, 2300 RA Leiden, The Netherlands

1 Introduction

This paper deals with collocation methods for the computation of periodic solutions to autonomous *delay differential equations* (DDEs),

$$\frac{dx(t)}{dt} = f(x(t), x(t - \tau)), \quad (1)$$

with one (constant) delay $\tau > 0$ and $f : \mathbb{R}^n \times \mathbb{R}^n \rightarrow \mathbb{R}^n$. For the sake of convenience we restrict ourselves to one-delay DDEs, but generalisation to multiple delays is straightforward.

Let $C := C([- \tau, 0], \mathbb{R}^n)$ be the vector space of continuous functions mapping the interval $[- \tau, 0]$ into \mathbb{R}^n . For $s \in \mathbb{R}$, denote by $x_s \in C$ the segment of a solution x to (1) defined by

$$x_s(\theta) = x(s + \theta), \quad \theta \in [- \tau, 0].$$

C is the state space for (1), that is, for any given s the solution segment x_s uniquely determines, via (1), the values $x(t)$ for all $t \geq s$. Consequently, any periodic solution to (1) can be found as the solution of the following *two-point boundary value problem* (BVP),

$$\begin{cases} \frac{dx(t)}{dt} = f(x(t), x(t - \tau)), & t \in [0, T] \\ x_0 = x_T \\ p(x, T) = 0, \end{cases} \quad (2)$$

where T denotes the (unknown) period and $p(x, T) = 0$ represents a suitable phase condition to remove translational invariancy.

Observe that the boundary condition $x_0 = x_T$ in (2) concerns a condition in an *infinite-dimensional* space, viz. C . This is clearly in contrast with the analogous problem for the case of ordinary differential equations (ODEs, i.e., equations (1) without a delay argument $x(t - \tau)$), where the boundary condition applies in a *finite-dimensional* space, \mathbb{R}^n .

In [21] the convergence of numerical simulations to stable periodic solutions was considered. In [26] a shooting approach is used, based on a combination of [15] and [25], for solving problem (2). This approach has been used to study a number of specific applications of DDEs [13, 12] and has been shown to be reasonably efficient.

The approach we follow in this paper is to solve the BVP (2) by the well known collocation method. Collocation methods are popular methods for the numerical solution of BVPs for systems of ODEs. The widely used COLSYS/COLNEW [1, 5] and AUTO [11] software packages employ collocation with piecewise polynomials to approximate the solutions to BVPs for ODEs. As far as we know, no prior work concerning the application of the method of collocation (not based on approximations by truncated Fourier series as in [10, 9, 32]) for solving BVPs of the kind (2) exists. Furthermore, theoretical convergence results from the current literature on the numerical solution of BVPs for DDEs do not appear to be applicable in the case of (2). We discuss this issue in section 2.

In this paper, our main aim is to study, by means of numerical experiments, a number of related collocation schemes for (2) with respect to their (observed) convergence orders and efficiency. In section 3 we outline the general setting relevant to collocation methods. In section 4 we review known convergence results concerning the numerical solution of IVPs for DDEs, which we will compare with the outcomes of our numerical experiments for the periodic BVP (2). This comparison is motivated by the fact that in the case of ODEs the same convergence orders are valid for similar discretisations of IVPs and BVPs, respectively. Next, in section 5 we explain the collocation variants that we investigate. In section 6 we describe the test models which we use, and we present our actual numerical results in section 7. Section 8 contains conclusions.

2 Two Kinds of Boundary Value Problems

A general two-point boundary value problem for delay differential equations (1) may be formulated as (cf., e.g., [17, 23])

$$\begin{cases} \frac{dx(t)}{dt} = f(x(t), x(t - \tau)), & t \in [0, T] \\ b(x_0, x_T) = 0, \end{cases} \quad (3)$$

where $b : C \times C \rightarrow C$ and $T > 0$ are given. However, in the current literature on the numerical solution of BVPs for DDEs (or more general functional differential equations), see, e.g., [4, 7, 3, 8, 29, 24] and [2, §11.7], one invariably encounters BVPs for (1) of the form

$$\begin{cases} \frac{dx(t)}{dt} = f(x(t), x(t - \tau)), & t \in [0, T] \\ x(\theta) = \phi(\theta), & \theta \in [-\tau, 0) \\ b(x(0), x(T)) = 0. \end{cases} \quad (4)$$

Here, an initial function $\phi \in C$ is given, a discontinuity in the solution at $t = 0$ is allowed, and $b : \mathbb{R}^n \times \mathbb{R}^n \rightarrow \mathbb{R}^n$ specifies a boundary condition in the finite-dimensional space \mathbb{R}^n . We note that both kinds of BVPs, (3) and (4), may contain additional conditions and corresponding free parameters (cf. $p(x, T) = 0$ and T in (2)). In [23] problem (3) is called Halanay's boundary value problem, whereas (4) is called a BVP with finite defect.

The existing literature on the numerical solution of BVPs for DDEs seems to be mainly targeted towards problems of the kind (4), which arise, amongst others, in control applications. We are not aware of theoretical convergence results on the numerical solution of the more general problem (3). Note that, in general, periodic solutions of (1) cannot be found as solutions to BVPs of the form (4).

3 Preliminaries

Below, we give our basic notations and the general setting relevant to collocation methods.

Let Π be a *mesh*, i.e., a collection of *mesh points* $0 = t_0 < t_1 < \dots < t_L = T$ which partition the interval $[0, T]$. Set $h_i := t_{i+1} - t_i$ for $i = 0, \dots, L-1$. Denote by π_m the set of all (vector-valued) polynomials of degree not exceeding m . We will approximate a solution x to (1) on the interval $[0, T]$ by an element from the following space of piecewise polynomials

$$S_m(\Pi) := \{u \in C([0, T], \mathbb{R}^n) : u|_{[t_i, t_{i+1}]} \in \pi_m, i = 0, \dots, L-1\}.$$

Clearly, $\dim S_m(\Pi) = n \times (L \times m + 1)$. Let

$$X(\Pi) := \bigcup_{i=0}^{L-1} X_i$$

with

$$X_i := \{c_{i,l} := t_i + c_l h_i, l = 1, \dots, m\}$$

be a given set of (so called) *collocation points* in $[0, T]$ based on the given, fixed set of *collocation parameters* $\{c_l\}$ with $0 \leq c_1 < c_2 < \dots < c_m \leq 1$. Then the idea of a *collocation method* for approximating a solution to the DDE (1) is to find a function $u : [-\tau, T] \rightarrow \mathbb{R}^n$, the so called *collocation solution*, such that: a) its restriction to $[0, T]$ belongs to $S_m(\Pi)$, b) for $i = 0, \dots, L-1$ its restriction to $[t_i, t_{i+1}]$ satisfies system (1) on the (finite) set X_i , and c) it fulfils the relevant initial or boundary value condition.

For $i = 0, \dots, L-1$ the collocation solution can be represented on subinterval $[t_i, t_{i+1}]$ as

$$u(t) = \sum_{j=0}^m u(t_{i+\frac{j}{m}}) P_{i,j}(t), \quad (5)$$

where

$$P_{i,j}(t) = \prod_{r=0, r \neq j}^m \frac{t - t_{i+\frac{r}{m}}}{t_{i+\frac{j}{m}} - t_{i+\frac{r}{m}}}, \quad j = 0, \dots, m \quad (6)$$

are Lagrange polynomials and

$$t_{i+\frac{j}{m}} = t_i + \frac{j}{m} h_i, \quad j = 1, \dots, m-1$$

are so called *representation points*. Thus the collocation solution u is completely determined on $[0, T]$ by the vectors $u_{i+\frac{j}{m}} := u(t_{i+\frac{j}{m}})$, $i = 0, \dots, L-1$, $j = 0, \dots, m-1$ and $u_L = u(t_L)$.

4 Initial Value Problems

In this section we consider the initial value problem

$$\begin{cases} \frac{dx(t)}{dt} = f(x(t), x(t-\tau)), & t \in [0, T] \\ x_0 = \phi, \end{cases} \quad (7)$$

where $\phi \in C$ is a given initial function.

Even if both f and ϕ are arbitrarily smooth, a solution x to (7) may have a discontinuity in its first derivative at $t = 0$. This is because in general

$$\left. \frac{d\phi(\theta)}{d\theta} \right|_{\theta=0^-} \neq f(\phi(0), \phi(-\tau)).$$

Due to the presence of the delayed term $x(t - \tau)$ in (7), the discontinuity at $t = 0$ is propagated forward in time. However, the discontinuity is smoothed as time increases, and a discontinuity in the $(k + 1)$ -th derivative of x , in general, appears at $t = k\tau$, $k = 0, 1, 2, \dots$. In a numerical procedure for IVPs (7) it is important to include some of these so called breaking points $t = k\tau$, $k = 0, 1, 2, \dots$, in the mesh to avoid a deterioration in the order of accuracy.

The theory concerning the numerical solution of IVPs for DDEs is well developed. Below several main results on the convergence behaviour of collocation methods in the case of the IVP (7) are collected. In particular, these deal also with collocation methods that are based on the well known *Gauss-Legendre* collocation parameters $\{c_l\}$, i.e. the roots of the m -th degree Gauss-Legendre polynomial transformed to $[0, 1]$.

The collocation method as outlined in section 3 consists in solving successively for $i = 0, \dots, L - 1$ the following system of equations for u restricted to $[t_i, t_{i+1}]$,

$$\frac{du(c_{i,l})}{dt} = \begin{cases} f(u(c_{i,l}), \phi(c_{i,l} - \tau)) & \text{when } c_{i,l} - \tau \leq 0 \\ f(u(c_{i,l}), u(c_{i,l} - \tau)) & \text{when } c_{i,l} - \tau > 0 \end{cases} \quad (8)$$

for $l = 1, \dots, m$, where $u(0) = \phi(0)$. The derivative of u in (8) has to be interpreted such that if $c_{i,l} = t_i$ it denotes the right derivative at t_i , whereas if $c_{i,l} = t_{i+1}$ it stands for the left derivative at t_{i+1} .

For ease of presentation, we assume in the rest of this section that all breaking points in $[0, T]$ are included in the mesh Π , and further, that f, ϕ are both arbitrarily smooth. We set $h := \max_i(h_i)$ and let $\|\cdot\|$ denote a given, fixed norm on \mathbb{R}^n .

The first theorem is a standard convergence result.

Theorem 4.1 *Let x be the exact solution to (7), and let u be a corresponding collocation solution as described in section 3 and above. Then the following estimate holds,*

$$\max_{t \in [0, T]} \|u(t) - x(t)\| = \mathcal{O}(h^m) \quad (h \downarrow 0). \quad (9)$$

If $\{c_l\}$ are the Gauss-Legendre collocation parameters, then the above estimate can be sharpened to

$$\max_{t \in [0, T]} \|u(t) - x(t)\| = \mathcal{O}(h^{m+1}) \quad (h \downarrow 0). \quad (10)$$

The following result deals with the special case where the mesh Π is such that for each $i < L$ with $t_i \geq \tau$ the subinterval $[t_i, t_{i+1}]$ is mapped by $t \mapsto t - \tau$ onto a (previous) subinterval $[t_k, t_{k+1}]$ with $0 \leq k < i$. A mesh with this property is called a *constrained mesh*.

Theorem 4.2 *Let x be the exact solution to (7), and let u be a corresponding collocation solution, as described in section 3 and above, based on a constrained mesh Π . If $\{c_l\}$ are the Gauss-Legendre collocation parameters, then the following estimate is valid,*

$$\max_{i=0,\dots,L} \|u(t_i) - x(t_i)\| = \mathcal{O}(h^{2m}) \quad (h \downarrow 0). \quad (11)$$

The above result can be found in [6, 16]. It means that *superconvergence* at the mesh points, a well known phenomenon in the case of both IVPs and BVPs for ODEs, also occurs in the case of IVPs for DDEs under an appropriate choice of Π .

The result of theorem 4.2 can be obtained for more general meshes Π when one considers application of alternative interpolation procedures in the past, instead of using the relevant local collocation polynomial. We state convergence theorems for two alternative types of interpolation procedures, where we leave the detailed (interpolation) formulas to section 5.1. We assume that the ratios h_{i+1}/h_i are uniformly bounded from below and above by fixed positive real numbers.

Let $q \geq 1$ be a given fixed integer. The first theorem below deals with the case of polynomial interpolation w.r.t. the mesh points for approximating the delayed term $x(t - \tau)$ (cf. (22)).

Theorem 4.3 *Let x be the exact solution to (7), and let u be a corresponding collocation solution, where in (8) the quantity $u(c_{i,l} - \tau)$ is replaced by the interpolating polynomial of degree q at $t = c_{i,l} - \tau$ that interpolates u at $q + 1$ mesh points t_j in the neighbourhood of t . If $\{c_l\}$ are the Gauss-Legendre collocation parameters, then the following estimates hold:*

$$\max_{i=0,\dots,L} \|u(t_i) - x(t_i)\| = \mathcal{O}(h^{\min(2m, q+1)}) \quad (h \downarrow 0), \quad (12)$$

$$\max_{t \in [0, T]} \|u(t) - x(t)\| = \mathcal{O}(h^{\min(m+1, q+1)}) \quad (h \downarrow 0). \quad (13)$$

Theorem 4.3 follows from common estimation arguments. If the above polynomial interpolation procedure is used with $q = 2m - 1$, superconvergence at the mesh points is obtained for (in essence) arbitrary meshes.

The next theorem deals with the case of *equistage* interpolation [19, 20] for approximating the delayed term (cf. (23)). At present, a satisfactory convergence analysis for this procedure, relevant to arbitrary meshes, is not known. A first result was obtained in [20].

Theorem 4.4 *Let x be the exact solution to (7), and let u be a corresponding collocation solution, where in (8) the quantity $u(c_{i,l} - \tau)$ is replaced by the equistage interpolating polynomial of degree q at $t = c_{i,l} - \tau$ that interpolates u at $q + 1$ points $c_{j,l}$ in the neighbourhood of t . If $\{c_l\}$ are the Gauss-Legendre collocation parameters, then (13) holds, and (12) holds under a model assumption on Π (see [20]).*

Result (12) follows from a direct application of the convergence theorem proved in [20]. The result concerning (13) can be shown using well known arguments.

We remark that if the mesh is constrained, then the collocation process described in theorem 4.4 reduces to the original collocation process, as in this case equistage interpolation is not actually performed. Thus, in this case theorems 4.1, 4.2 apply.

5 Computation of Periodic Solutions

In this section we explain in detail the collocation variants that we consider. We also discuss the structure of the linear system which needs to be solved in each Newton iteration and describe adaptive mesh selection.

5.1 Outline of the Collocation Variants

For our numerical method, it is convenient to consider instead of BVP (2) a transformed BVP that is obtained from (2) after scaling time by the factor T^{-1} ,

$$\begin{cases} \frac{dx(t)}{dt} = Tf(x(t), x(t - \frac{\tau}{T})), & t \in [0, 1] \\ x_0 = x_1 \\ p(x, T) = 0. \end{cases} \quad (14)$$

In the following we assume that $\tau < T$. We set $\bar{\tau} = \tau T^{-1}$. Note that a periodic solution to (1) is arbitrarily smooth for all times (if f is arbitrarily smooth). Therefore no time points have to be included in the mesh a priori, cf. section 4.

A collocation solution u to the transformed BVP (14), corresponding to a mesh Π on $[0, 1]$ and collocation parameters $\{c_l\}$, is determined (cf. section 3) in terms of the unknowns

$$u_{i+\frac{j}{m}} = u(t_{i+\frac{j}{m}}), \quad i = 0, \dots, L-1, \quad j = 0, \dots, m-1 \quad \text{and} \quad u_L = u(t_L)$$

by the *collocation equations*

$$\frac{du(c_{i,l})}{dt} = \begin{cases} Tf(u(c_{i,l}), u(c_{i,l} - \bar{\tau} + 1)) & \text{when } c_{i,l} - \bar{\tau} < 0, \\ Tf(u(c_{i,l}), u(c_{i,l} - \bar{\tau})) & \text{when } c_{i,l} - \bar{\tau} \geq 0 \end{cases} \quad (15)$$

for $i = 0, \dots, L-1, l = 1, \dots, m$. Here, the same convention on the derivative of u holds as in the case of (8).

Clearly, for BVP (2) the initial function, x_0 , is not known beforehand. But, the periodic boundary condition is linear, and in constructing (15) we have used this fact in order to eliminate directly the numerical unknowns corresponding to times $t < 0$. We did not eliminate u_0 (because its value is used to determine u in $[0, t_1]$), so we still need to require

$$u_0 = u_L, \quad (16)$$

together with the phase condition

$$p(u, T) = 0. \quad (17)$$

In order to solve the combined nonlinear system (15), (16), (17), we apply Newton iteration. Write $c = c_{i,l}$ and

$$\tilde{c} = \begin{cases} c - \bar{\tau} + 1 & \text{when } c - \bar{\tau} < 0, \\ c - \bar{\tau} & \text{when } c - \bar{\tau} \geq 0. \end{cases} \quad (18)$$

Let integer k be such that $t_k \leq \tilde{c} < t_{k+1}$. Then (15) assumes the form

$$\sum_{j=0}^m u_{i+\frac{j}{m}} P'_{i,j}(c) = Tf\left(\sum_{j=0}^m u_{i+\frac{j}{m}} P_{i,j}(c), \sum_{j=0}^m u_{k+\frac{j}{m}} P_{k,j}(\tilde{c})\right), \quad (19)$$

where $P'_{i,j}$ denotes the derivative of $P_{i,j}$. After linearisation of (19) w.r.t. u, T we obtain

$$\begin{aligned} & \sum_{j=0}^m P'_{i,j}(c) \Delta u_{i+\frac{j}{m}} - f(u(c), u(\tilde{c})) \Delta T - TA_0(u(c), u(\tilde{c})) \sum_{j=0}^m P_{i,j}(c) \Delta u_{i+\frac{j}{m}} \\ & - TA_1(u(c), u(\tilde{c})) \left(\sum_{j=0}^m P_{k,j}(\tilde{c}) \Delta u_{k+\frac{j}{m}} + \left(\sum_{j=0}^m u_{k+\frac{j}{m}} P'_{k,j}(\tilde{c}) \right) \frac{\tau}{T^2} \Delta T \right) \\ & = - \left(\sum_{j=0}^m u_{i+\frac{j}{m}} P'_{i,j}(c) - Tf(u(c), u(\tilde{c})) \right) \end{aligned} \quad (20)$$

where

$$u(c) = \sum_{j=0}^m u_{i+\frac{j}{m}} P_{i,j}(c), \quad u(\tilde{c}) = \sum_{j=0}^m u_{k+\frac{j}{m}} P_{k,j}(\tilde{c})$$

and

$$A_0(\xi, \eta) = \frac{\partial f}{\partial \xi}(\xi, \eta), \quad A_1(\xi, \eta) = \frac{\partial f}{\partial \eta}(\xi, \eta).$$

Note that (19) is, through \tilde{c} , in general nondifferentiable with respect to T whenever $t_k = \tilde{c}$. We have (arbitrarily) chosen the right derivative when this occurs. The nondifferentiability can deteriorate the asymptotic quadratic convergence of the Newton iteration. However, since periodic solutions have continuous derivatives, we did not expect nor encountered problems in our test cases.

We also deal with two variants to the above collocation scheme. Here, the value of the collocation solution at \tilde{c} (“in the past”),

$$u(\tilde{c}) = \sum_{j=0}^m u_{k+\frac{j}{m}} P_{k,j}(\tilde{c}), \quad (21)$$

is replaced, in (19), by the value of an interpolating polynomial of (fixed) degree $q = k_1 + k_2$ constructed through $q + 1$ mesh points in the neighbourhood of \tilde{c} ,

$$u(\tilde{c}) \rightarrow \sum_{j=k-k_1}^{k+k_2} u(t_j) Q_{k,j}(\tilde{c}), \quad (22)$$

or, by the value of an interpolating polynomial defined according to equistage interpolation (see [19], [20]),

$$u(\tilde{c}) \rightarrow \sum_{j=k-k_1}^{k+k_2} u(c_{j,l}) R_{k,j,l}(\tilde{c}), \quad (23)$$

where

$$Q_{k,j}(t) = \prod_{r=k-k_1, r \neq j}^{k+k_2} \frac{t - t_r}{t_j - t_r}, \quad R_{k,j,l}(t) = \prod_{r=k-k_1, r \neq j}^{k+k_2} \frac{t - c_{r,l}}{c_{j,l} - c_{r,l}}. \quad (24)$$

Integers k_1, k_2 are chosen such that the points t_j and $c_{j,l}$ lie centred around the value $\tilde{c} \in [t_k, t_{k+1}]$. Remark that, if the mesh points or collocation points used in (22), (23), (24) have indices outside $0, \dots, L$ they are appropriately substituted using 'periodic continuation' of Π and u (as in (18)).

5.2 Linear System Structure

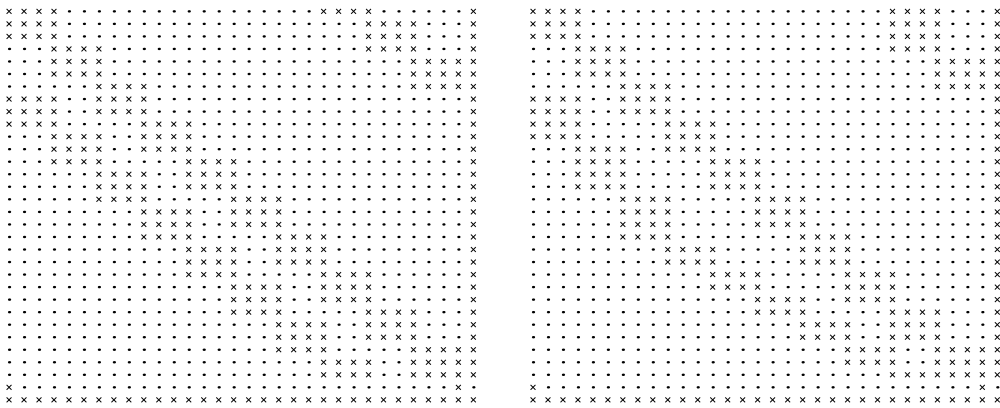


Figure 1: Structure of the matrix arising in the Newton iteration in the case of method (16),(17),(19) and model (29) using a uniform mesh (left) and a non-uniform mesh (right) with $L = 10$ and collocation polynomials of degree $m = 3$ ($n = 1, \tau = 1, T \approx 4.0964$). Zero elements are indicated by dots (\cdot) and nonzero elements by crosses (\times).

Figure 1 visualises the structure of two matrices corresponding to two cases of the system of linear equations (20), (16), (17), which defines the Newton iteration. These matrices contain a (large) $mLn \times (mL + 1)n$ block filled with two (circular) bands. This block is bordered by one column and $n + 1$ rows. The extra column contains derivatives with respect to the period; n extra rows contain condition (16), and one extra row arises because of the phase condition (17).

The diagonal band is itself a concatenation of $mn \times (m + 1)n$ blocks. The off-diagonal band is a consequence of the delay term, its circularity is due to the (eliminated) periodicity condition. When the mesh is equidistant (uniform), the off-diagonal band lies at a fixed distance from the diagonal band. This distance is approximately equal to $\bar{\tau}$ of the total matrix size. When the mesh is non-uniform, this distance changes (see figure 1, (right)).

In the case of ordinary differential equations, the linear system can be solved with a band solver. Then the band size is proportional to the system size n and the (polynomial) degree m but it does not depend on the number of intervals L . For delay differential equations this is no longer possible. For moderate values of

m , n and L the linear system can be solved with a direct method as we did in our tests. Efficiency could be increased using, e.g., a chord-Newton method, in which case the Jacobian is not recomputed (and factored) in every iteration but remains fixed during a number of iterations.

Figure 2 shows the structure of the matrices corresponding to the linearised system of equations for the collocation variants defined by the replacements (22) and (23), respectively. As can be seen, both variants yield an increase in the size of the bandwidth of the off-diagonal band, approximately by a factor q .

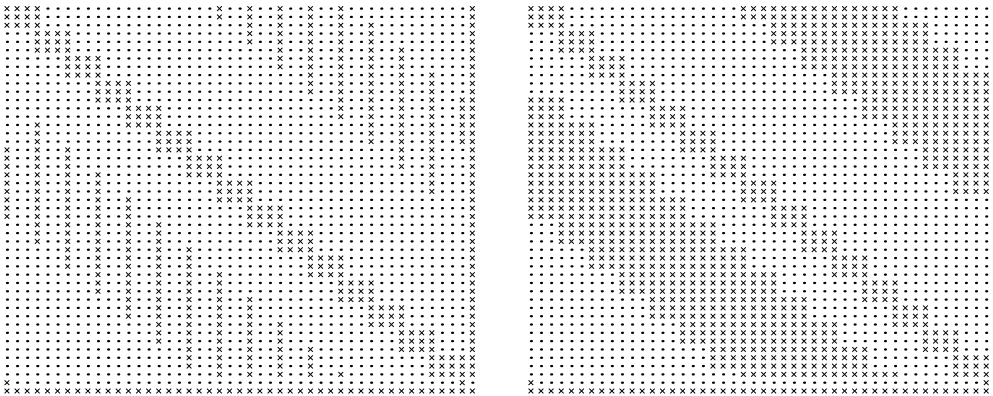


Figure 2: Structure of the matrices arising in the Newton iteration in the case of collocation variants based on (22) (left) and (23) (right) for model (27) using a uniform mesh with $L = 15$, collocation polynomials of degree $m = 3$, and $q = 5$ ($n = 1$, $\tau = 2$, $T \approx 5.3918$). Zero elements are indicated by dots (\cdot), and nonzero elements by crosses (\times).

We conclude this subsection by noticing that the technique of condensation of parameters (cf. [2]) cannot be applied in our case except for the collocation variant based on (22) because its interpolation procedure in the past only uses approximations at the mesh points.

5.3 Adaptive Mesh Selection

Adaptive mesh selection for BVPs for ordinary differential equations is achieved by equidistributing the integral

$$K = \int_0^1 |x^{(m+1)}(Ts)|^{\frac{1}{m+1}} ds,$$

over the mesh intervals,

$$\int_{t_i}^{t_{i+1}} |x^{(m+1)}(Ts)|^{\frac{1}{m+1}} ds = \frac{1}{L} K, \quad i = 0, \dots, L-1, \quad (25)$$

where $x(t)$ is scalar and $|\cdot|$ is the absolute value, see, e.g., [11, 2].

The new mesh points, t_i , satisfying (25) are determined using an approximation of $x^{(m+1)}$ obtained from the current mesh and collocation solution u .

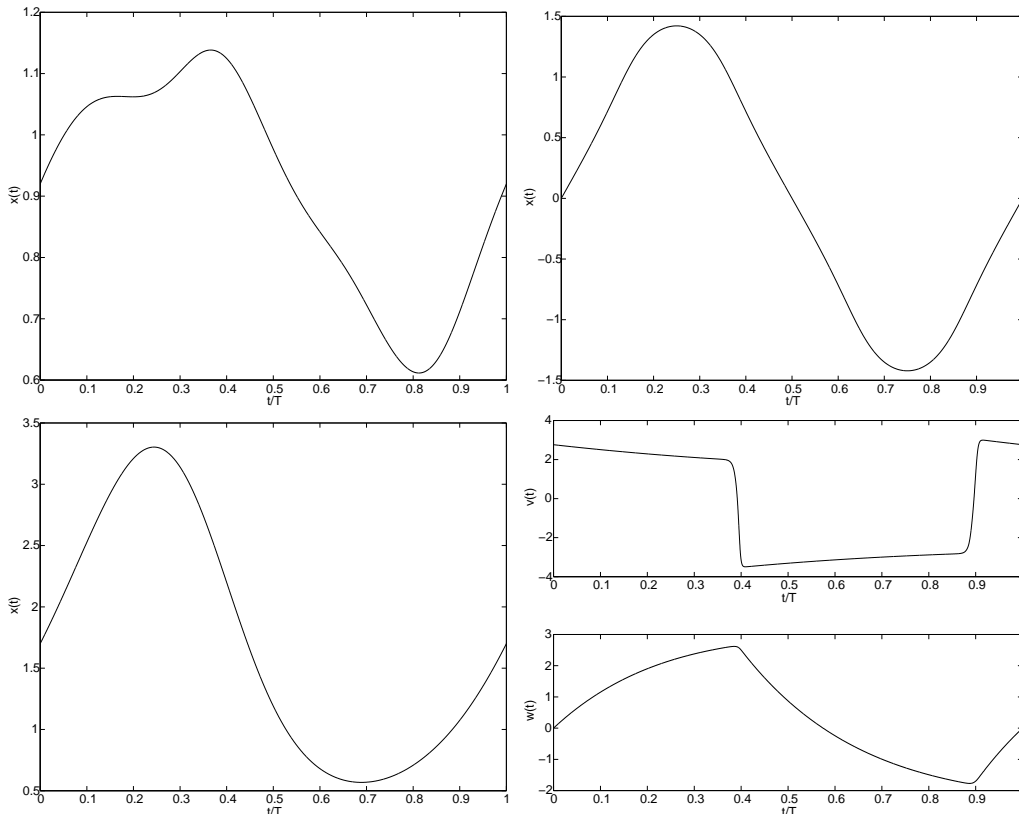


Figure 3: The periodic solutions under consideration: model 1 (upper left), 2 (upper right), 3 (lower left) and 4 (lower right).

Formula (25) is based on the error estimate

$$|x(tT) - u(t)| = Ch_i^{m+1} \max_{s \in [t_i, t_{i+1}]} |x^{(m+1)}(Ts)| + \mathcal{O}(h^{m+2}), \quad t \in [t_i, t_{i+1}], \quad (26)$$

when using Gauss-Legendre collocation points. Formula (26) is proven for BVPs for ordinary differential equations using a Green's function [30]. The use of a Green's function can be extended to BVPs of finite defect (4) (see [4] which includes a discussion of its changed smoothness properties) but the approach is not applicable to the 'infinite-dimensional' BVP (3). Hence the validity of (26) remains an important open question in our situation.

Our numerical tests (see section 7.2), however, indicate that formula (26) remains valid for the periodic BVP (2). We subsequently implemented and tested the strategy (25) as implemented in AUTO on the models considered in this paper. These tests resulted in a desirable decrease in error for difficult profiles (compared to the use of a uniform mesh of the same size) but in an increase in error for rather easy profiles (i.e. profiles without steep gradients). The latter phenomenon (which did not disappear even for very fine meshes) was, after a number of tests, removed by changing the discretisation formula used for (25) in AUTO to the trapezium rule.

The scheme then showed both (small) decrease in error for easy profiles and (even larger than before) decrease in error for difficult profiles. We conclude with the formulae for the latter variant.

Based on the old mesh points, t_i , and the piecewise constant $u^{(m)}$, let

$$d_i = \frac{u^{(m)}(\xi_{i+1}) - u^{(m)}(\xi_i)}{\frac{1}{2}(t_{i+1} - t_{i-1})}, \quad i = 0, \dots, L,$$

where $\xi_i \in (t_{i-1}, t_i)$, $\xi_{i+1} \in (t_i, t_{i+1})$ are chosen arbitrarily and where 'periodic continuation' is used for d_0 and d_L . We approximate

$$S(t) = \int_0^t |x^{(m+1)}(Ts)|^{\frac{1}{m+1}} ds$$

by $\tilde{S}(t)$ at the old mesh points using $\tilde{S}(t_0) = 0$ and

$$\tilde{S}(t_{i+1}) = \tilde{S}(t_i) + (t_{i+1} - t_i) \frac{|d_i|^{\frac{1}{m+1}} + |d_{i+1}|^{\frac{1}{m+1}}}{2}, \quad i = 1, \dots, L - 1,$$

and assume \tilde{S} is linear between mesh points. If u is not scalar, \tilde{S} is computed for each component as above and then summed over all components. The new t_i 's are now easily selected from the monotonically increasing \tilde{S} by linear interpolation such that $t_0 = 0$ and $\tilde{S}(t_{i+1}) - \tilde{S}(t_i) = \Delta\tilde{S} = \frac{\tilde{S}(1)}{L}$, $i = 1, \dots, L$.

6 Test Models

In this section we formulate the models we considered to test the collocation methods described in section 5. The periodic solution profiles (scaled to the interval $[0, 1]$) are displayed in figure 3.

Model 1 The following equation is a model for the regeneration of white blood cells [14, 18] and is usually referred to as the Mackey-Glass equation,

$$\frac{dx}{dt} = ax(t) + b \frac{x(t - \tau)}{1 + x^c(t - \tau)}, \quad (27)$$

where a , b , c , τ are given parameters. For $a = -1$, $b = 1.74$, $c = 10$, $\tau = 2$ we computed an unstable periodic solution with period $T \approx 5.3918$.

Model 2 The scalar delay differential equation

$$\frac{dx}{dt} = \alpha x(t - 1) \frac{1 + x^2(t - 1)}{1 + x^4(t - 1)} \quad (28)$$

was studied analytically (see, e.g., [22, 27, 31]) and numerically [15, 10, 26]. It was proven that at $\alpha = \pi/2$ a family of periodic solutions bifurcates from the zero solution and that stable periodic solutions of period $T = 4$ exist whenever $\alpha > \pi/2$. Here we consider such a stable periodic solution at $\alpha = 2$.

Model 3 This is the well known delayed logistic equation

$$\frac{dx}{dt} = (\lambda - x(t-1))x(t), \quad (29)$$

cf., e.g., [17, 21]. We computed a stable periodic solution at $\lambda = 1.7$ with $T \approx 4.0964$.

Model 4 The following system models recurrent neural feedback [28, 9],

$$\begin{cases} \frac{dv}{dt} = h(v(t)) - w(t) + I(v(t - \tau)), \\ \frac{dw}{dt} = \rho(v(t) + a - bw(t)) \end{cases} \quad (30)$$

with

$$\begin{cases} h(v) = v - v^3/3, \\ I(v) = \mu(v - v_0), \\ v_0 = \text{the unique real root of } h(v_0) - (v_0 + a)/b + I(v_0). \end{cases}$$

This system exhibits a stable spiked periodic solution for parameter values $a = 0.7$, $b = 0.8$, $\rho = 0.08$, $\tau = 25$, $v_0 \approx -1.1994$ and $\mu = -2$ with $T \approx 50.7326$.

7 Results

In this section we discuss our numerical results. For a given mesh Π we compute (approximations of) the *continuous error* E_C and the *discrete error* E_I , defined by

$$E_C = \max_{t \in [0,1]} \|x(Tt) - u(t)\|, \quad E_I = \max_{i=0, \dots, L} \|x(Tt_i) - u(t_i)\|,$$

where x denotes the exact periodic solution, u denotes a collocation solution, and $\|\cdot\|$ is the Euclidean norm. To this purpose, we first computed a reference solution for x , using $L = 1000$ subintervals. Next, we compared the reference solution to u (for $L = 10, \dots, 200$) at a very fine mesh in order to compute E_C , and at (only) the mesh points in order to compute E_I . As a phase condition, we fixed the value of one component of the solution at $t_0 = 0$. We show observed orders of convergence and the results of adaptive mesh selection.

7.1 Numerical Order Results

In this subsection the mesh points are always taken equidistant, i.e., $h_i = h$ for $i = 1, \dots, L$.

First we concentrate on the collocation method (16), (17), (19). Figure 4 shows the evolution of E_C and E_I for collocation solutions with $m = 4$ as h goes to zero using equidistant collocation points (collocation parameters $\{c_l\} = \{\frac{1}{8}, \frac{3}{8}, \frac{5}{8}, \frac{7}{8}\}$) (left) and Gauss-Legendre collocation points (right). Clearly, an $\mathcal{O}(h^m)$ versus $\mathcal{O}(h^{m+1})$ convergence behaviour is apparent. We have approximated the slope of the graph of the continuous error E_C by means of a least squares fit on (all) the results for $L = 100, \dots, 200$. Table 1 summarises the obtained convergence orders of E_C for

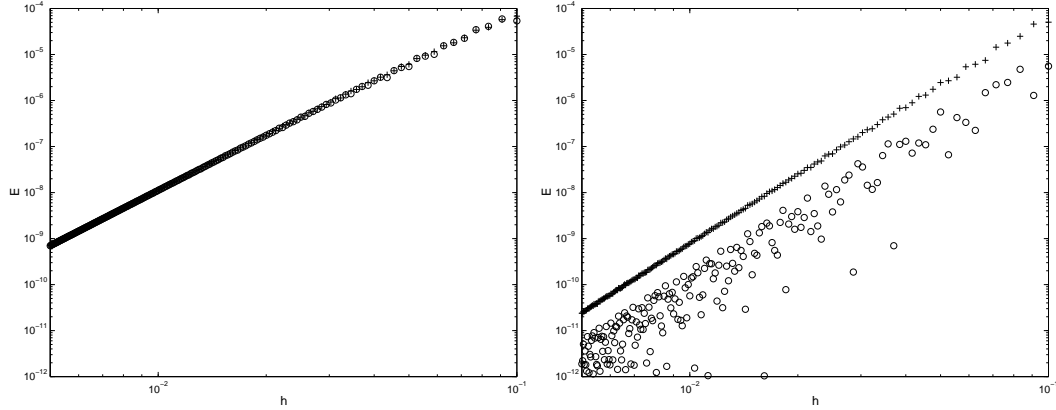


Figure 4: Evolution of E_C (+) and E_I (o) in the case of model 1 and the collocation method (16),(17),(19) with $m = 4$ using equidistant (left) and Gauss-Legendre (right) collocation points.

$m = 2, 3, 4$. For odd m , a numerical convergence behaviour of $\mathcal{O}(h^{m+1})$ is also found in the case of equidistant collocation points. This feature seems to be a consequence of the specific choice of the collocation parameters and it disappears if they are not chosen symmetrically with respect to $1/2$. The table clearly shows agreement with the result of theorem 4.1 for IVPs for DDEs (and with results for BVPs of the form (4), see [4, 7]).

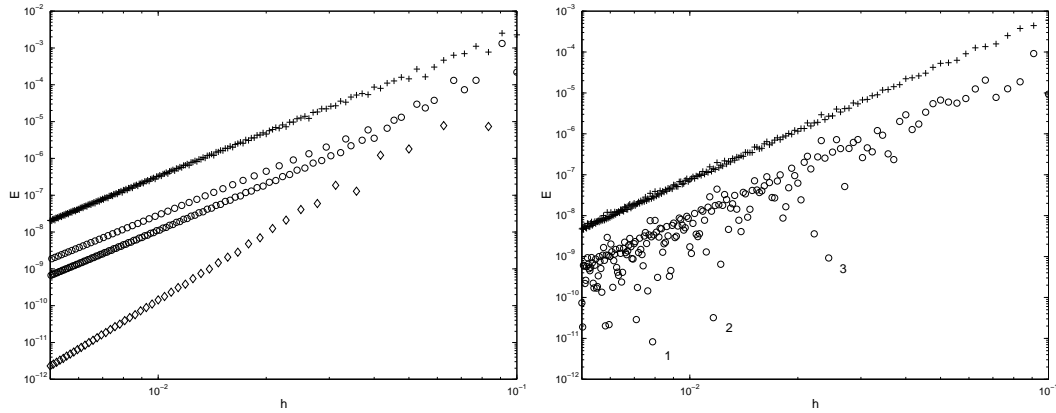


Figure 5: Evolution of E_C (+) and E_I (o and \diamond) for models 2 (left) and 3 (right) based on the collocation method (16), (17), (19) with $m = 3$ and Gauss-Legendre collocation points. Left: superconvergence of E_I when L is a multiple of 4 (E_I indicated as a \diamond). Right: greater accuracy for E_I when $\frac{\tau}{T}L \approx 31.003$ (1), $\frac{\tau}{T}L \approx 20.994$ (2), $\frac{\tau}{T}L \approx 10.009$ (3).

Superconvergence at mesh points is not present in the E_I curve of figure 4 (right). According to theorem 4.2 it is recovered in the case of IVPs for DDEs for constrained meshes. The special situation that mesh points get mapped into mesh points (and collocation points into collocation points) by the delay depends, for BVPs, both on the model and the mesh [2]. More specifically, it occurs when $k\tau = lT$ with k and

m	model 1	model 2	model 3	m	model 1	model 2	model 3
2	2.016	2.042	2.004	2	2.992	3.004	3.003
3	4.008	4.009	3.980	3	4.003	3.999	4.001
4	4.003	4.017	4.033	4	5.003	4.990	4.927

Table 1: Approximations to the orders of convergence of E_C in the case of models 1–3 and the collocation method (16), (17), (19) for $L = 100, \dots, 200$ using equidistant (left) and Gauss-Legendre (right) collocation points.

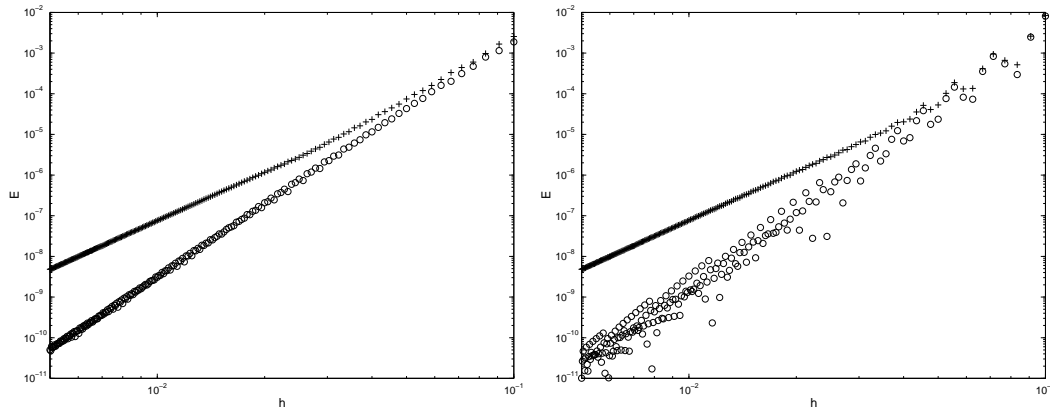


Figure 6: Evolution of E_C (+) and E_I (o) for model 3 based on collocation variants (22) (left) and (23) (right) with $m = 3$, $q = 2m - 1$ and Gauss-Legendre collocation points.

l integer and (equidistant) mesh points with L a multiple of k . This is the case for model 2 where $4\tau = T$ whenever L is a multiple of 4. During computations, this relation holds only approximately as T is computed with finite accuracy. Nevertheless we numerically observe superconvergence, see figure 5 (left). We further observe that, when the period and the delay are not commensurate, E_I is generally smaller whenever L is such that $\frac{\tau}{T}L$ is near an integer number (that is, whenever L is a multiple of k and $\frac{\tau}{T} \approx \frac{l}{k}$ for some k, l), see figure 5 (right).

m	model 1	model 2	model 3
2	4.009	3.991	4.020
3	5.900	5.736	5.980
4	7.776	7.379	7.814

Table 2: Approximation to the orders of convergence of E_I for models 1-3 using collocation solutions based on collocation variant (22) with $L = 50, \dots, 100$ and Gauss-Legendre collocation points.

We now consider the two variants of the collocation method (16), (17), (19) where, instead of using the collocation solution in the past, the interpolation formula (22) or (23) is applied. Figure 6 shows the evolution of E_C and E_I when $u(\tilde{c})$ is replaced by an interpolating polynomial of degree $q = 2m - 1$ through $q + 1$ mesh points t_j according to (22) (left), or through $q + 1$ collocation points $c_{j,l}$ according

to (23) (right). The obtained convergence orders for E_I in the case of the variant based on (22) are summarised in table 2. In both cases, we observe superconvergence behaviour for E_I , which is in agreement with theorems 4.3, 4.4. Further, if h is sufficiently small, both variants have essentially the same continuous error E_C as the original collocation method, cf. figures 5 (right) and 6.

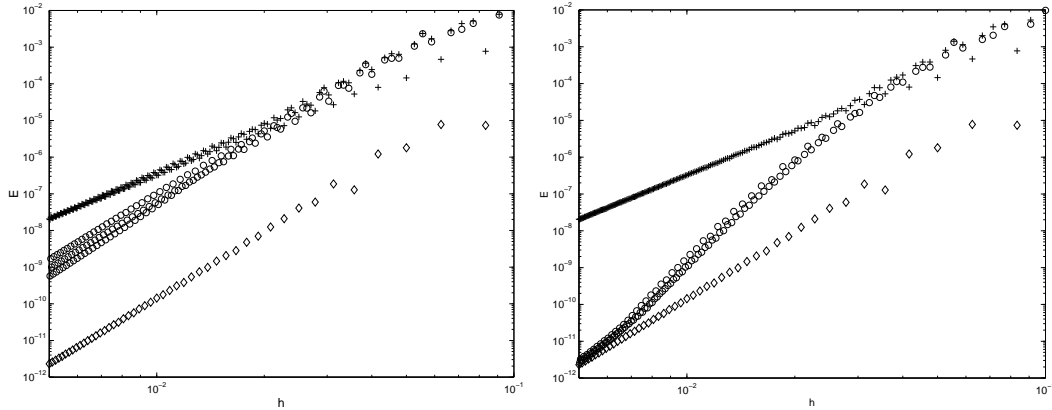


Figure 7: Evolution of E_C (+) and E_I (\diamond when L is a multiple of 4, \circ otherwise) for model 2 based on collocation variant (23) with $m = 3$, $q = 2m - 1$ (left) respectively $q = 2m + 3$ (right) and Gauss-Legendre collocation points.

Though, for E_I , $\mathcal{O}(h^{2m})$ is the maximum order of convergence, we observed that, for the collocation variants, E_I can be further decreased for small h by choosing $q > 2m - 1$. This is illustrated in figure 7 (compare left to right for points where L is not a multiple of 4).

7.2 Adaptive Mesh Selection

When the mesh is uniform formula (26) implies that the error is locally proportional to the $(m + 1)$ -th derivative of the solution profile. This correspondence is clearly visible in figure 8 and was observed in several other tests as well.

On profiles without steep gradients (figure 3, models 1-3) little benefit can be expected from an adapted mesh in comparison with a uniform mesh. However, as mentioned in section 5.3, AUTO's adaptive mesh selection can, at times, increase the error for the case of DDEs. This unfavourable feature does not disappear as h goes to zero, see figure 9 (top). Instead, it was (almost completely) removed by slightly changing the scheme as described in section 5.3. We might also note that we did not observe this feature in a small number of tests on periodic solutions of ordinary differential equations.

The periodic solution of model 4 exhibits steep gradients and we successfully used adaptive mesh selection to decrease the errors significantly. Here too, the variant described in section 5.3 gives better results (see figure 9 (bottom)). The evolution, for this example, of both E_C and E_I versus L are shown in figure 10. Note that an increase of more than three orders of accuracy is gained by adapting the mesh

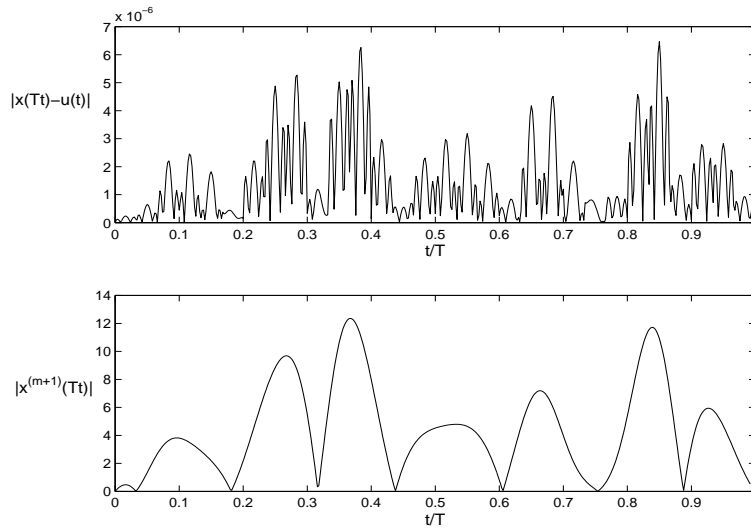


Figure 8: Correspondence of the error $|x(Tt) - u(t)|$ and the $(m + 1)$ -th derivative, $|x^{(m+1)}(Tt)|$, of a collocation solution for model 1 using $m = 3$, $L = 30$, a uniform mesh and Gauss-Legendre collocation points.

compared to the accuracy using a uniform mesh with the same number of intervals and thus the same number of unknowns in the Newton procedure.

As a last remark, we note that when adaptive mesh selection is applied in the case of model 4 and the collocation variants based on (22) or (23), errors decrease compared to uniform meshes but not as much as in figure 10. Also, no superconvergence was visible within the range of intervals computed.

We conclude that our numerical results indicate for the collocation method (16), (17), (19) the validity of formula (26) and approach (25) combined with the need for a (small) change in their discretisation used in a practical implementation.

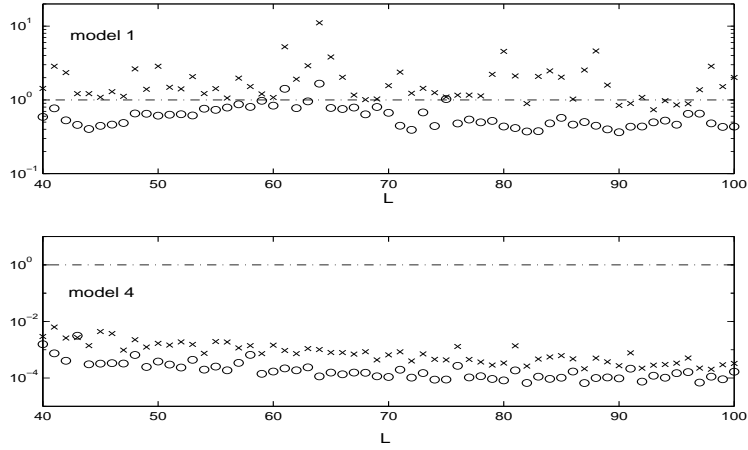


Figure 9: Ratio $E_C^{\text{adapted}}(L)/E_C^{\text{uniform}}(L)$ versus L using AUTO's adaptive mesh selection (\times) respectively the variant described in section 5.3 (\circ) for $L = 40, \dots, 100$. Here, $m = 3$ and Gauss-Legendre collocation points are used to compute the collocation solutions for model 1 (upper part) and model 4 (lower part).

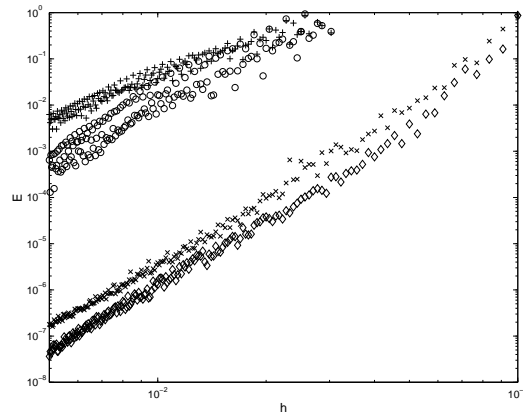


Figure 10: Evolution of E_C ($+$, \times) and E_I (\circ , \diamond) for model 4 using equidistant ($+$, \circ) respectively adapted (\times , \diamond) meshes with $m = 3$ and Gauss-Legendre collocation points.

8 Conclusions

Collocation, based on piecewise polynomials, is considerably successful in the numerical solution of (periodic) BVPs for systems of ordinary differential equations. It is, e.g., used in the software packages COLSYS/COLNEW [1, 5] and AUTO [11]. In this paper we investigated the use of collocation methods for computing periodic solutions to delay differential equations.

We studied three collocation methods, two of which are based on alternative interpolation procedures for approximating the delayed term. The presence of the delayed term influences the structure of the linear system to be solved in the Newton iteration and thus affects the efficiency of the collocation method. Based on an extensive set of numerical tests we obtained information on the order of convergence and its dependence on the collocation discretisation. We show how these results correspond with known convergence results for initial value problems for DDEs. In particular, we show when superconvergence at mesh points is lost and/or recovered. We end with a brief discussion of adaptive mesh selection.

Acknowledgements

This research presents results of the Research Project OT 98/16 and the Fellowship F/98/68, funded by the Research Council K.U.Leuven and of the research project IUAP P4/02 funded by the programme on Interuniversity Poles of Attraction, initiated by the Belgian State, Prime Minister's Office for Science, Technology and Culture. The scientific responsibility is assumed by its authors. K. Engelborghs is a research assistant of the Fund for Scientific Research - Flanders.

References

- [1] U. M. Ascher, J. Christiansen, and R. D. Russell. Collocation software for boundary value ODEs. *ACM Trans. Math. Software*, 7:209–222, 1981.
- [2] U. M. Ascher, R. M. M. Mattheij, and R. D. Russell. *Numerical Solution of Boundary Value Problems for Ordinary Differential Equations*. Prentice Hall, 1988.
- [3] N. V. Azbelev, V. P. Maksimov, and L. F. Rakhmatullina. *Introduction to the Theory of Functional Differential Equations*. Nauka, Moscow, 1991. (in Russian).
- [4] G. Bader. Solving boundary value problems for functional differential equations by collocation. In U. M. Ascher and R. D. Russell, editors, *Numerical Boundary Value ODEs*, volume 5 of *Progress in Scientific Computing*, pages 227–243. Birkhäuser Boston, 1985.

- [5] G. Bader and U. M. Ascher. A new basis implementation for a mixed order boundary value ode solver. *SIAM J. Sci. Stat. Comp.*, 8:483–500, 1987.
- [6] A. Bellen. One-step collocation for delay differential equations. *J. Comput. Appl. Math.*, 10:275–283, 1984.
- [7] A. Bellen. A Runge-Kutta-Nystrom method for delay differential equations. *Progress in Scientific Computing*, 5:271–283, 1985.
- [8] A. Bellen and M. Zennaro. A collocation method for boundary value problems of differential equations with functional arguments. *Computing*, 32:307–318, 1984.
- [9] A. M. Castelfranco and H. W. Stech. Periodic solutions in a model of recurrent neural feedback. *SIAM J. Appl. Math.*, 47(3):573–588, 1987.
- [10] E. J. Doedel and P. P. C. Leung. A numerical technique for bifurcation problems in delay differential equations. *Congr. Num.*, 34:225–237, 1982.
- [11] E. J. Doedel, X. J. Wang, and T. F. Fairgrieve. AUTO94: Software for continuation and bifurcation problems in ordinary differential equations. Technical Report CRPC-95-2, Center for Research on Parallel Computing, California Institute of Technology, Pasadena, USA, 1995.
- [12] K. Engelborghs, V. Lemaire, J. Bélair, and D. Roose. Numerical bifurcation analysis of delay differential equations arising from physiology modeling. In preparation, 1999.
- [13] K. Engelborghs, D. Roose, and T. Luzyanina. Bifurcation analysis of periodic solutions of neutral functional differential equations: a case study. *Internat. J. Bifur. Chaos*, 8(10):1889–1905, 1998.
- [14] L. Glass and M. C. Mackey. Oscillation and chaos in physiological control systems. *Science*, 197:287–289, 1977.
- [15] K. P. Hadeler. Effective computation of periodic orbits and bifurcation diagrams in delay equations. *Numer. Math.*, 34:457–467, 1980.
- [16] E. Hairer, S. P. Nørsett, and G. Wanner. *Solving ordinary differential equations I. Nonstiff problems*, volume 8 of *Springer series in computational mathematics*. Springer-Verlag, 2nd edition, 1993.
- [17] J. K. Hale. *Theory of Functional Differential Equations*, volume 3 of *Applied Mathematical Sciences*. Springer-Verlag, 1977.
- [18] J. K. Hale and N. Sternberg. Onset of chaos in differential delay equations. *J. Comput. Phys.*, 77:221–239, 1988.

- [19] K. J. in 't Hout. A new interpolation procedure for adapting Runge-Kutta methods to delay differential equations. *BIT*, 32:634–649, 1992.
- [20] K. J. in 't Hout. Convergence of Runge-Kutta methods for delay differential equations. Technical Report TW-98-11, Rijksuniversiteit Leiden, Afdeling Wiskunde en Informatica, February 1999. Submitted for publication.
- [21] K. J. in 't Hout and Ch. Lubich. Periodic orbits of delay differential equations under discretization. *BIT*, 38(1):72–91, 1998.
- [22] J. L. Kaplan and J. A. Yorke. Ordinary differential equations which yield periodic solutions of differential delay equations. *J. Math. Anal. Appl.*, 48:317–324, 1974.
- [23] V. B. Kolmanovskii and A. Myshkis. *Introduction to the theory and application of functional differential equations*, volume 463 of *Mathematics and its applications*. Kluwer Academic Publishers, 1999.
- [24] X. Liu. Periodic boundary value problems for differential equations with finite delay. *Dynam. Systems Appl.*, 3:357–368, 1994.
- [25] K. Lust, D. Roose, A. Spence, and A. Champneys. An adaptive Newton-Picard algorithm with subspace iteration for computing periodic solutions. *SIAM J. Sci. Comput.*, 19(4):1188–1209, 1998.
- [26] T. Luzyanina, K. Engelborghs, K. Lust, and D. Roose. Computation, continuation and bifurcation analysis of periodic solutions of delay differential equations. *Internat. J. Bifur. Chaos*, 7(11):2547–2560, 1997.
- [27] R. D. Nussbaum. Periodic solutions of nonlinear autonomous functional differential equations. In H.-O. Peitgen and H.-O. Walther, editors, *Functional Differential Equations and Approximation of Fixed Points*, volume 730 of *Lecture Notes in Mathematics*, pages 283–325. Springer-Verlag, 1978.
- [28] R. E. Plant. A FitzHugh differential-difference equation modeling recurrent neural feedback. *SIAM J. Appl. Math.*, 40(1):150–162, February 1981.
- [29] G. W. Reddien and C. C. Travis. Approximation methods for boundary value problems of differential equations with functional arguments. *J. Math. Anal. Appl.*, 46:62–74, 1974.
- [30] R. D. Russell and J. Christiansen. Adaptive mesh selection strategies for solving boundary value problems. *SIAM J. Numer. Anal.*, 15(1):59–80, 1978.
- [31] H.-O. Walther. A theorem on the amplitudes of periodic solutions of differential delay equations with application to bifurcation. *J. Diff. Eqns.*, 39:369–404, 1978.

- [32] A. Zapp. Verzweigungseigenschaften bei nichtlinearen Differentialgleichungen mit einer Zeitverzögerung. Diplomarbeit, University of Cologne, 1997.